arXiv:1401.3095v2 [quant-ph] 10 Sep 2014

Coupling spin ensembles via superconducting flux qubits

Yueyin Qiu,[1,2] Wei Xiong,[1] Lin Tian,[3] and J. Q. You[2,*]

[1]*Department of Physics, Fudan University, Shanghai 200433,China*
[2]*Beijing Computational Science Research Center, Beijing 100084, China*
[3]*School of Natural Sciences, University of California, Merced, California 95343, USA*

(Dated: September 11, 2014)

We study a hybrid quantum system consisting of spin ensembles and superconducting flux qubits, where each spin ensemble is realized using the nitrogen-vacancy centers in a diamond crystal and the nearest-neighbor spin ensembles are effectively coupled via a flux qubit. We show that the coupling strengths between flux qubits and spin ensembles can reach the strong and even ultrastrong coupling regimes by either engineering the hybrid structure in advance or tuning the excitation frequencies of spin ensembles via external magnetic fields. When extending the hybrid structure to an array with equal coupling strengths, we find that in the strong-coupling regime, the hybrid array is reduced to a tight-binding model of a one-dimensional bosonic lattice. In the ultrastrong-coupling regime, it exhibits quasi-particle excitations separated from the ground state by an energy gap. Moreover, these quasi-particle excitations and the ground state are stable under a certain condition that is tunable via the external magnetic field. This may provide an experimentally accessible method to probe the instability of the system.

PACS numbers: 03.67.Ac, 42.50.Dv, 85.25.Cp, 76.30.Mi

I. INTRODUCTION

As an important subfield in quantum information, quantum simulation [1] has attracted increasing interest, and considerable advancements were achieved both theoretically [2–7] and experimentally [8–12]. Recently, hybrid quantum systems [13–25] have been strongly recommended for quantum simulation because they can combine two distinct advantages of the subsystems: the tunability of artificial atoms such as quantum circuits, and the long coherence times of atoms or spins. Also, strong and tunable coupling between two subsystems can be realized via either direct [19, 26–28] or indirect [29–31] coupling schemes.

Among various hybrid quantum systems, the one consisting of superconducting qubits and nitrogen-vacancy (NV) centers in a diamond crystal [29, 30] has become a topic of current interest. This hybrid quantum system has the merits of high tunability and scalability in superconducting qubits, and long coherence times and stable energy levels in NV centers. In addition, the magnetic coupling between superconducting qubits and NV centers can be stronger than that between NV centers and a transmission line resonator [29] by three orders of magnitude. These distinct advantages make this hybrid system a good candidate for simulating the abundant features of many-body systems. For instance, a hybrid quantum architecture composed of inductively coupled flux qubits, where a NV-center ensemble is placed on top of each qubit loop, was proposed [32] to simulate a Jaynes-Cummings (JC) lattice. Using this hybrid quantum system, it is possible to investigate the quantum phase transition between the localized and delocalized phases in a Bose-Hubbard-like model. Because the flux qubits and the NV centers can be tuned by external magnetic fields, the JC lattice simulated using them is simpler and more tunable than those realized using coupled cavities [33–37].

In this paper, we study hybrid quantum systems consisting of spin ensembles and superconducting flux qubits, where each spin ensemble is also realized using the NV centers in a diamond crystal. Different from the hybrid quantum system in Ref. [32], a flux qubit is placed in between two NV-center ensembles, and every two nearest-neighbor spin ensembles are effectively coupled via this flux qubit. The coupling strength between flux qubits and spin ensembles can be tuned to reach the strong- and even ultrastrong-coupling regimes by either engineering the hybrid structure in advance or tuning the excitation frequencies of spin ensembles via the external magnetic fields. These hybrid quantum systems can be used to simulate the systems of coupled bosons, including the demonstration of bilinear coupling among the bosons. Moreover, these hybrid systems have the advantage of scalability, so they can be extended to construct hybrid arrays to simulate one-dimensional (1D) bosonic lattices with tunable coupling strengths. In the strong-coupling regime, the hybrid array is simply reduced to the tight-binding model of a 1D bosonic lattice. In the ultrastrong-coupling regime, the hybrid array exhibits more interesting properties. For instance, because of the bilinear coupling in this regime, it can exhibit quasi-particle excitations that have an energy gap from the ground state. Moreover, it is found that these quasi-particle excitations and the ground state are stable under a certain condition that is tunable via the external magnetic field. This may provide an experimentally accessible method to probe the instability of the system.

*Electronic address: jqyou@csrc.ac.cn

The paper is organized as follows. In Sec. II, we describe the proposed hybrid quantum system consisting of two flux qubits and three adjoining spin ensembles. The effective Hamiltonian for the spin ensembles is derived in Sec. III by adiabatically eliminating the degrees of freedom of the flux qubits in the dispersive regime. In Sec. IV, the proposed hybrid quantum system is extended to a hybrid array, so as to simulate 1D bosonic lattices with tunable coupling strengths. The behavior of this system in both the strong- and the ultrastrong- coupling regimes is studied. Finally, discussions and conclusions are given in Sec. V.

II. THE PROPOSED HYBRID QUANTUM SYSTEM

We start from the simple structure consisting of three spin ensembles, with every two nearest-neighbor ensembles coupled by a flux qubit [see Fig. 1(a)]. We use NV centers in a diamond crystal as a spin ensemble [22]. Each flux qubit is realized by a superconducting loop interrupted with three Josephson junctions and biased by a static external magnetic field perpendicular to the loop [38]. This superconducting qubit can have a superposition state of clockwise and counterclockwise persistent currents in the loop. In contrast to the previous proposals [29, 30], where a NV-center ensemble is placed inside the loop of a flux qubit, we place a flux qubit in between two NV-center ensembles in order to achieve effective coupling of the NV-center ensembles and scalable hybrid structures.

For a NV center, the spin-1 triplet sublevels of its electronic ground state with $m_{\rm s}=0$ and $m_{\rm s}=\pm1$ have a zero-field splitting [see Fig. 1(b)]. Because the strain-induced splitting is negligible compared to the Zeeman splitting, the electronic ground state of a single NV center can be described by [39]

$$H_{\rm NV}=DS_z^2+g_e\mu_B\mathbf{B}\cdot\mathbf{S}, \tag{1}$$

where D is the zero-field splitting of the electronic ground state, $\mathbf{S}$ is the usual spin-1 operator, g_e is the g-factor, and μ_B is the Bohr magneton. For convenience, we set the crystalline axis of the NV center as the z direction. As shown in Fig. 1(b), by introducing a weak external magnetic field $B_z^{\rm ext}$ along the z direction, an additional Zeeman splitting between $m_s=\pm1$ sublevels occurs. Thus, a two-level quantum system with sublevels $m_s=0$ and -1 can be separated from the other levels. In the subspace of this two-level system, the Hamiltonian of a single NV center can be reduced to (we set $h=1$)

$$H_{\rm NV}=\frac{1}{2}\nu_s\tau_z, \tag{2}$$

where $\nu_s=D-g_e\mu_B B_z^{\rm ext}$ is the energy difference between the lowest two sublevels with $m_s=0$ and -1, and $\tau\equiv(\tau_x,\tau_y,\tau_z)$ denote the Pauli operators with the two basis states corresponding to the lowest two sublevels.

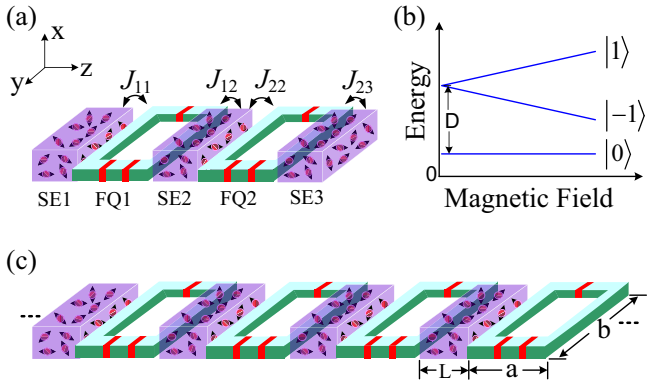

FIG. 1: (Color online) (a) Schematic diagram of the proposed hybrid quantum system. Among the three spin ensembles, every two nearest-neighbor spin ensembles are coupled by a superconducting flux qubit. The qubit loop is on the y-z plane and perpendicular to the x direction. (b) The Zeeman splitting for the spin-1 sublevels $m_{\rm s}=0,\pm1$ of the electronic ground state in a NV center. (c) Hybrid array consisting of spin ensembles and flux qubits, which is a periodic extension of the hybrid quantum system in (a).

The subsystem of two flux qubits has a Hamiltonian as follows [40]

$$H_{\rm FQ}=\sum_{i=1}^{2}\frac{1}{2}(\varepsilon_i\sigma_z^{(i)}+\lambda_i\sigma_x^{(i)})+M_{12}\sigma_z^{(1)}\sigma_z^{(2)}, \tag{3}$$

where the first two terms involve two isolated flux qubits and the third one is the interaction Hamiltonian of the two flux qubits coupled via a mutual inductance m_{12} defined by $M_{12}=m_{12}I_p^{(1)}I_p^{(2)}$, with $I_p^{(i)}$ being the persistent current of the ith flux qubit; $\varepsilon_i=2I_p^{(i)}(\Phi^{(i)}-\Phi_0/2)$ is the energy bias of the ith flux qubit (where $\Phi^{(i)}$ is the applied static magnetic flux, and Φ_0 the flux quantum), λ_i is the tunneling energy, and $\boldsymbol{\sigma}\equiv(\sigma_x^{(i)},\sigma_y^{(i)},\sigma_z^{(i)})$ denote the Pauli operators of the ith flux qubit. To reduce the effect of the flux noise, the external static magnetic field of each flux qubit is biased at the degeneracy point with $\varepsilon_i=0$, so that the transition frequency is $\nu_{qi}=\lambda_i$.

Note that the two persistent-current states of each flux qubit can produce an additional static magnetic field. This magnetic field leads to couplings between the flux qubit and its two neighboring NV centers. In the following discussions, we use the eigenstates of $\sigma_x^{(i)}$ as the new basis states with $\sigma_x^{(i)}\to\sigma_z^{(i)}$, and $\sigma_z^{(i)}\to\sigma_x^{(i)}$. Then, the Hamiltonian of the hybrid quantum system in Fig. 1(a)

can be written as [21, 32]

$$H=\sum_{i=1}^{2}\frac{1}{2}\nu_{qi}\sigma_z^{(i)}+M_{12}\sigma_x^{(1)}\sigma_x^{(2)}+\sum_{j=1,2,3}\sum_{m=1}^{n}\frac{1}{2}\nu_s^{(m)}\tau_{z,j}^{(m)}$$
$$+\sum_{m=1}^{n}[J_{11}^{(m)}(\tau_{1,+}^{(m)}+\tau_{1,-}^{(m)})\sigma_x^{(1)}+J_{12}^{(m)}(\tau_{2,+}^{(m)}+\tau_{2,-}^{(m)})\sigma_x^{(1)}$$
$$+J_{22}^{(m)}(\tau_{2,+}^{(m)}+\tau_{2,-}^{(m)})\sigma_x^{(2)}+J_{23}^{(m)}(\tau_{3,+}^{(m)}+\tau_{3,-}^{(m)})\sigma_x^{(2)}], \quad (4)$$

where $J_{ij}^{(m)}\equiv\frac{1}{\sqrt{2}}g_e\mu_B B_{ij}^{(m)}$ is the coupling strength between the ith flux qubit and the mth NV center in the jth spin ensemble, with $B_{ij}^{(m)}$ ($i=1,2; j=1,2,3$) being the corresponding magnetic field in the x direction generated by the ith flux qubit acting on the mth NV center in the jth spin ensemble. The central spin ensemble (i.e., the second one) experiences the magnetic fields generated by both the left and right neighboring flux qubits.

To describe the collective excitation of each spin ensemble, one can define

$$s_j^\dagger=\frac{1}{J_{ij}}\sum_{m=1}^{n}J_{ij}^{(m)}\tau_{j,+}^{(m)}, \quad (5)$$

where

$$J_{ij}=\sqrt{\sum_m|J_{ij}^{(m)}|^2}. \quad (6)$$

In the condition of large n and low excitations for each spin ensemble, $s_j^\dagger$ and s_j satisfies the bosonic commutation relation $[s_j,s_j^\dagger]\approx 1$ (see, e.g., [32, 41, 42]). Using these collective operators, the total Hamiltonian in Eq. (4), can be rewritten as

$$H=H_{\rm FQ}+H_{\rm SE}+H_{\rm SE-FQ} \quad (7)$$

with

$$\begin{aligned}H_{\rm FQ}&=\frac{1}{2}\nu_{q1}\sigma_z^{(1)}+\frac{1}{2}\nu_{q2}\sigma_z^{(2)}+M_{12}\sigma_x^{(1)}\sigma_x^{(2)},\\ H_{\rm SE}&=\nu_{s1}s_1^\dagger s_1+\nu_{s2}s_2^\dagger s_2+\nu_{s3}s_3^\dagger s_3,\\ H_{\rm SE-FQ}&=J_{11}(s_1^\dagger+s_1)\sigma_x^{(1)}+J_{12}(s_2^\dagger+s_2)\sigma_x^{(1)}\\ &\quad+J_{22}(s_2^\dagger+s_2)\sigma_x^{(2)}+J_{23}(s_3^\dagger+s_3)\sigma_x^{(2)}.\end{aligned} \quad (8)$$

Below we estimate the coupling strength J_{ij}. The superconducting loop of each flux qubit can be designed as, e.g., a rectangular loop with length b and width a, where the narrow side with a is along the z direction and the nearest-neighbor flux qubits are separated by L, i.e., the width of the diamond crystal placed in between two adjoining flux qubits [see Fig. 1(c)]. Therefore, we can denote the position of a NV center located on the symmetric line along the z direction of the nearest-neighbor rectangular loops as $z_{\rm NV}$, where $0\le z_{\rm NV}<L$. According to the Biot-Savart law, the magnetic field generated by the left flux qubit acting on this NV center can be written as

$$B(z_{\rm NV})=\frac{\mu_0 I_p}{\pi}\Big\{\frac{1}{\sqrt{(b/2)^2+(a+z_{\rm NV})^2}}\times\Big[\frac{z_{\rm NV}+a}{b}+\frac{b}{4(z_{\rm NV}+a)}\Big]-\frac{1}{\sqrt{(b/2)^2+z_{\rm NV}^2}}\Big(\frac{b}{4z_{\rm NV}}+\frac{z_{\rm NV}}{b}\Big)\Big\}, \quad (9)$$

where μ_0 is the magnetic permeability. The corresponding coupling $J^{(m)}(z_{\rm NV})=\frac{1}{\sqrt{2}}g_e\mu B^{(m)}(z_{\rm NV})$, produced by the left flux qubit on this NV center, is shown in Fig. 2. Here we choose the magnetic field $\bar{B}$ at $z_{\rm NV}/L=0.5$ as the average magnetic field [21, 30] to estimate the coupling produced by the left qubit on its adjoining NV-center ensemble, i.e., $J=\sqrt{\frac{n}{2}}g_e\mu\bar{B}$. From Fig. 2, it can be seen that the coupling for a single NV center decreases slightly when $z_{\rm NV}$ shifts from $z_{\rm NV}/L=0.5$ to approaching 1 (i.e., close to the right flux qubit), but increases drastically when $z_{\rm NV}$ changes from $z_{\rm NV}/L=0.5$ to approaching 0 (i.e., close to the left flux qubit). Thus, it is expected that the actual coupling produced by the flux qubit on its adjoining NV-center ensemble should be larger than J.

To estimate the value of the coupling J, we choose the experimentally accessible density of NV centers as

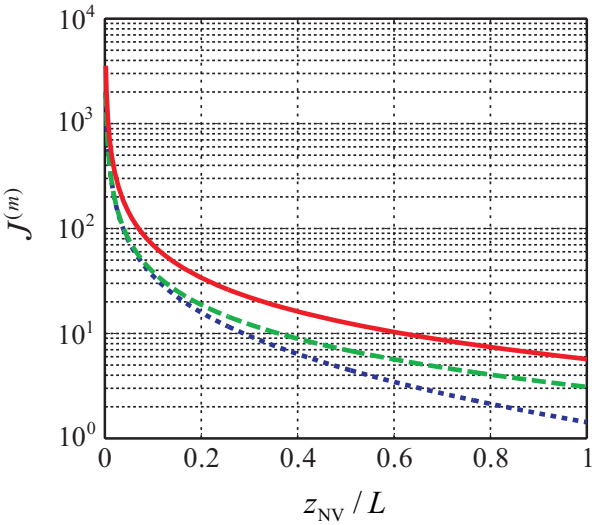

FIG. 2: (Color online) The separation ($z_{\rm NV}$) dependence of the coupling strength $J^{(m)}$ between the flux qubit and the mth spin in the NV-center ensemble, which is located on the symmetric line of the rectangular loop in the z direction. Here $I_p^{(i)}=0.5$ μA, and $a=b=1$ μm for the (blue) dotted curve; $I_p^{(i)}=0.5$ μA, $a=2$ μm, and $b=10$ μm for the (green) dashed curve; and $I_p^{(i)}=0.9$ μA, $a=2$ μm, and $b=50$ μm for the (red) solid curve.

3×10^6 μm^{-3} [43], the height of the diamond crystal as 5 μm, and the thickness of the superconducting loop as 60 nm [29]. For persistent current $I_p^{(i)}=0.5$ μA, $a=b=1$ μm, and $L=0.5$ μm, we have $J\approx\sqrt{n}J^{(m)}\sim$ 13 MHz. When a is increased to 2 μm and b to 10 μm, $J\sim60$ MHz. This reaches the strong coupling regime since the coupling strength produced by the flux qubit on its adjoining NV-center ensemble is larger than the decoherence rates of both the flux qubit ($\gamma_{\rm FQ}\sim1$ MHz) and the NV center ensemble ($\gamma_{\rm SE}\sim10$ MHz [30]). When $I_p^{(i)}$ is increased to $I_p^{(i)}=0.9$ μA [44], and b to 50 μm, the coupling J is strengthened to $J\sim250$ MHz, which can be comparable to the excitation frequency ν_s of the NV-center ensemble because $\nu_s\equiv D-g_e\mu_B B_z^{\rm ext}$ can be tuned small via the external magnetic field. This corresponds to the ultrastrong coupling regime. As for the inductive coupling between the nearest-neighbor flux qubits, because they are separated by ~1 μm, it is as weak as $M_{12}\sim1-10$ MHz [45]. Therefore, compared to the coupling between the flux qubit and its adjoining NV-center ensemble, the inductive coupling can be neglected in the Hamiltonian (8).

III. EFFECTIVE HAMILTONIAN OF THE SPIN ENSEMBLES

We rewrite the Hamiltonian (7) as

$$H=H_0+H_{\rm I}, \tag{10}$$

where the free part H_0 is

$$H_0=\frac{1}{2}\nu_{q1}\sigma_z^{(1)}+\frac{1}{2}\nu_{q2}\sigma_z^{(2)}+\nu_{s1}s_1^\dagger s_1+\nu_{s2}s_2^\dagger s_2+\nu_{s3}s_3^\dagger s_3, \tag{11}$$

and the interaction part $H_{\rm I}$ is

$$\begin{aligned}H_I=&J_{11}(\sigma_-^{(1)}s_1^\dagger+\sigma_-^{(1)}s_1+{\rm H.c.})\\&+J_{12}(\sigma_-^{(1)}s_2^\dagger+\sigma_-^{(1)}s_2+{\rm H.c.})\\&+J_{22}(\sigma_-^{(2)}s_2^\dagger+\sigma_-^{(2)}s_2+{\rm H.c.})\\&+J_{23}(\sigma_-^{(2)}s_3^\dagger+\sigma_-^{(2)}s_3+{\rm H.c.}).\end{aligned} \tag{12}$$

We consider the large-detuning case with $\Delta_{ij}\gg J_{ij}$, where $\Delta_{ij}\equiv\nu_{qi}-\nu_{sj}>0$ ($i=1,2$; $j=1,2,3$). In such a case, the flux qubits can be regarded as being kept in their ground states and only virtual excitations can occur. Therefore, we can use the Fröhlich-Nakajima transformation [46–48] to adiabatically eliminate the degrees of freedom of flux qubits to obtain an effective coupling between the nearest-neighbor spin ensembles. This unitary transformation $U=\exp(-V)$ requires the anti-Hermitian operator $V=-V^\dagger$ to satisfy

$$H_{\rm I}+[H_0,V]=0. \tag{13}$$

This gives rise to an effective Hamiltonian, up to second order, as

$$H_{\rm eff}=UHU^\dagger=H_0+\frac{1}{2}[H_{\rm I},V]+O(J^3), \tag{14}$$

where the anti-Hermitian operator V has the following form:

$$\begin{aligned}V=&A_1(\sigma_-^{(1)}s_1^\dagger-\sigma_+^{(1)}s_1)+A_5(\sigma_-^{(1)}s_1-\sigma_+^{(1)}s_1^\dagger)\\&+A_2(\sigma_-^{(1)}s_2^\dagger-\sigma_+^{(1)}s_2)+A_6(\sigma_-^{(1)}s_2-\sigma_+^{(1)}s_2^\dagger)\\&+A_3(\sigma_-^{(2)}s_2^\dagger-\sigma_+^{(2)}s_2)+A_7(\sigma_-^{(2)}s_2-\sigma_+^{(2)}s_2^\dagger)\\&+A_4(\sigma_-^{(2)}s_3^\dagger-\sigma_+^{(2)}s_3)+A_8(\sigma_-^{(2)}s_3-\sigma_+^{(2)}s_3^\dagger),\end{aligned} \tag{15}$$

with the coefficients given by

$$\begin{aligned}A_1&=\frac{J_{11}}{\Delta_{11}},\quad A_2=\frac{J_{12}}{\Delta_{12}},\ A_3=\frac{J_{22}}{\Delta_{22}},\quad A_4=\frac{J_{23}}{\Delta_{23}},\\A_5&=\frac{J_{11}}{\Lambda_{11}},\quad A_6=\frac{J_{12}}{\Lambda_{12}},\quad A_7=\frac{J_{22}}{\Lambda_{22}},\quad A_8=\frac{J_{23}}{\Lambda_{23}}.\end{aligned} \tag{16}$$

Here $\Lambda_{ij}\equiv\nu_{qi}+\nu_{sj}$ ($i=1,2$; $j=1,2,3$).

Because the coefficients A_l ($l=1$ to 8) are small in the large-detuning case, the higher-order terms of the Fröhlich-Nakajima transformation can be dropped out and only the second-order term $[H_{\rm I},V]$ needs to be kept. Moreover, owing to the separate design of the nearest-neighbor flux qubits in our approach, the diagonal term of each flux qubit remains respectively at its original expectation value in the adiabatic approximation, i.e., $\sigma_z^{(i)}\longrightarrow\left\langle\sigma_z^{(i)}\right\rangle=-1$, with $i=1,2$. After eliminating the degrees of freedom of each flux qubit, the effective Hamiltonian can be obtained as

$$\begin{aligned}H_{\rm eff}=&\nu_1's_1^\dagger s_1+\nu_3's_3^\dagger s_3+\nu_2's_2^\dagger s_2-g_{11}(s_1^\dagger s_1^\dagger+s_1s_1)\\&-g_{22}(s_2^\dagger s_2^\dagger+s_2s_2)-g_{33}(s_3^\dagger s_3^\dagger+s_3s_3)\\&-g_{12}(s_1s_2^\dagger+s_2s_1^\dagger+s_2^\dagger s_1^\dagger+s_1s_2)\\&-g_{23}(s_2s_3^\dagger+s_3s_2^\dagger+s_3^\dagger s_2^\dagger+s_2s_3),\end{aligned} \tag{17}$$

where the parameters are given by

$$\begin{aligned}\nu_1'&=\nu_{s1}-2g_{11},\quad \nu_3'=\nu_{s3}-2g_{33},\\\nu_2'&=\nu_{s2}-J_{12}^2\Big(\frac{1}{\Delta_{12}}+\frac{1}{\Lambda_{12}}\Big)-J_{22}^2\Big(\frac{1}{\Delta_{22}}+\frac{1}{\Lambda_{22}}\Big),\\g_{11}&=\frac{J_{11}^2}{2}\Big(\frac{1}{\Delta_{11}}+\frac{1}{\Lambda_{11}}\Big),\quad g_{33}=\frac{J_{23}^2}{2}\Big(\frac{1}{\Delta_{23}}+\frac{1}{\Lambda_{23}}\Big),\\g_{22}&=\frac{J_{12}^2}{2}\Big(\frac{1}{\Delta_{12}}+\frac{1}{\Lambda_{12}}+\frac{1}{\Delta_{22}}+\frac{1}{\Lambda_{22}}\Big),\\g_{12}&=\frac{J_{11}J_{12}}{2}\Big(\frac{1}{\Delta_{12}}+\frac{1}{\Lambda_{12}}+\frac{1}{\Delta_{11}}+\frac{1}{\Lambda_{11}}\Big),\\g_{23}&=\frac{J_{22}J_{23}}{2}\Big(\frac{1}{\Delta_{23}}+\frac{1}{\Lambda_{23}}+\frac{1}{\Delta_{22}}+\frac{1}{\Lambda_{22}}\Big).\end{aligned} \tag{18}$$

Here ν_{si}' is the effective excitation frequency of the ith spin ensemble, and g_{12} (g_{23}) is the effective coupling strength between the first (second) and second

(third) spin ensembles. Therefore, we achieve an effective coupling between the nearest-neighboring spin ensembles, where each spin ensemble behaves like a boson. In Eq. (17), there are bilinear terms $s_i^\dagger s_i^\dagger + s_i s_i$ $(i = 1, 2, 3)$, which involve one-mode squeezing within the same bosons. Also, there are bilinear terms $s_2^\dagger s_1^\dagger + s_1 s_2$ and $s_3^\dagger s_2^\dagger + s_2 s_3$, which involve two-mode squeezing between the three different bosons. These terms become important in the ultrastrong coupling regime with $g_{ij} \sim \nu_j'$ $(i = 1, 2; j = 1, 2, 3)$.

As a special case, we further consider the strong coupling regime, i.e., $\gamma_{\rm FQ}, \gamma_{\rm SE} \ll J_{ij} \ll \Delta_{ij}$ and $g_{ij} \ll \nu_j'$. In this case, the rotating-wave approximation can be applied, and the effective Hamiltonian is reduced to

$$H_{\rm eff} = \nu_1' \, s_1^\dagger s_1 + \nu_2' s_2^\dagger s_2 + \nu_3' s_3^\dagger s_3 - g_{12}(s_2^\dagger s_1 + s_1^\dagger s_2) - g_{23}(s_3^\dagger s_2 + s_2^\dagger s_3), \quad (19)$$

where ν_i', g_{12}, and g_{23} are given in Eq. (18). As compared with Eq. (17), the effective Hamiltonian is now reduced to a JC form.

IV. HYBRID ARRAY

As an extension of the hybrid structure in Fig. 1(a), we now propose a hybrid array in Fig. 1(c). Here we consider a periodic system with $\nu_{sl} = \nu_s$, $g_{l,l+1} = g$, and the periodic boundary condition. Similar to Eq. (17), the effective Hamiltonian of the hybrid array can be written as

$$H = (\nu_s - 2g)\sum_j s_j^\dagger s_j - g\sum_j (s_j^\dagger s_j^\dagger + s_j s_j + s_j^\dagger s_{j+1} + s_{j+1}^\dagger s_j + s_j^\dagger s_{j+1}^\dagger + s_{j+1} s_j), \quad (20)$$

where

$$g = J^2\Big(\frac{1}{\Delta} + \frac{1}{\Lambda}\Big), \quad (21)$$

with $\Delta = \nu_q - \nu_s$, and $\Lambda = \nu_q + \nu_s$.

In order to diagonalize the Hamiltonian (20), instead of using the site operator $s_j^\dagger(s_j)$ acting on the jth spin ensemble, we employ the wave-vector operators $b_k^\dagger(b_k)$ acting on all ensembles in the array:

$$s_j^\dagger = \frac{1}{\sqrt{N}}\sum_k e^{-ik\cdot j} b_k^\dagger,$$
$$s_j = \frac{1}{\sqrt{N}}\sum_k e^{ik\cdot j} b_k, \quad (22)$$

where N is the number of spin ensembles in the array. The new collective operators present themselves like a wave excitation of bosons in the hybrid array. We Fourier

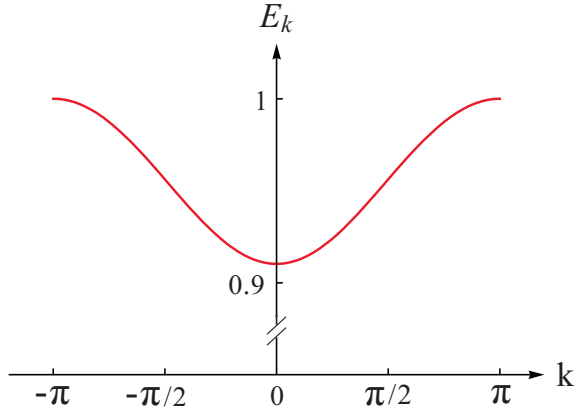

FIG. 3: (Color online) Dispersion relation for the quasi-particle energy E_k in Eq. (27), where $J = 0.25$ GHz, $\omega_q = 6$ GHz and $\omega_s = 1$ GHz. Note that an energy gap occurs, which separates the quasi-particle excitations from the ground state.

transform the bosonic operators to convert the Hamiltonian to

$$H = \sum_k \Big\{ [(\nu_s - 2g(1+\cos k)]\, b_k^\dagger b_k - g(1+e^{ik})(b_k^\dagger b_{-k}^\dagger + b_{-k} b_k) \Big\}, \quad (23)$$

with $-\pi \le k < \pi$. Because there are relations $b_k^\dagger b_{-k}^\dagger = b_{-k}^\dagger b_k^\dagger$ and $b_{-k} b_k = b_k b_{-k}$ for bosons, the Hamiltonian (23) can be rewritten as

$$H = \sum_k \Big\{ [\nu_s - 2g(1+\cos k)]\,(b_k^\dagger b_k + b_{-k}^\dagger b_{-k}) - 2g(1+\cos k)(b_k^\dagger b_{-k}^\dagger + b_{-k} b_k) \Big\}, \quad (24)$$

where $0 \le k < \pi$, i.e., the wave vector k is now confined in half of the first Brillouin zone.

Furthermore, we apply the Bogoliubov transformation:

$$b_k = \mu_k \alpha_k - \nu_k \alpha_{-k}^\dagger,$$
$$b_k^\dagger = \mu_k^* \alpha_k^\dagger - \nu_k^* \alpha_{-k},$$
$$b_{-k} = \mu_k \alpha_{-k} - \nu_k \alpha_k^\dagger,$$
$$b_{-k}^\dagger = \mu_k^* \alpha_{-k}^\dagger - \nu_k^* \alpha_k, \quad (25)$$

where $|\mu_k|^2 - |\nu_k|^2 = 1$. It is clear that α_k and $\alpha_k^\dagger$ also satisfy the bosonic commutation relations: $[\alpha_k, \alpha_{k'}^\dagger] = \delta_{kk'}$, and $[\alpha_k, \alpha_{k'}] = [\alpha_k^\dagger, \alpha_{k'}^\dagger] = 0$. Then, the Hamiltonian is diagonalized to

$$H = \sum_k E_k(\alpha_k^\dagger \alpha_k + \alpha_{-k}^\dagger \alpha_{-k}) + E_g, \quad (26)$$

where the quasi-particle energy is

$$E_k = \sqrt{\nu_s^2 - 4\nu_s g(1+\cos k)}, \quad (27)$$

and the ground-state energy is

$$E_g = \sum_k \Big\{ \sqrt{\nu_s^2 - 4\nu_s g(1+\cos k)} - [\nu_s - 2g(1+\cos k)] \Big\}. \tag{28}$$

Here the parameters are required to satisfy

$$\nu_s \geqslant 8g. \tag{29}$$

In the opposite limit with $\nu_s < 8g$, the eigenmodes contain imaginary solutions, and the system is unstable. This indicates that when the frequency detuning is fixed, the coupling strength J between the flux qubits and the spin ensembles should be bounded even in the ultrastrong regime, so as to achieve a stable quantum system. The dispersion relation for the quasi-particle energy E_k with the given parameters is shown in Fig. 3, where an energy gap separates the quasi-particle excitations from the ground state. Experimentally, one can tune $\nu_s \equiv D - g_e \mu_B B_z^{\rm ext}$ via the external magnetic field $B_z^{\rm ext}$ on the NV centers in order to satisfy the condition in Eq. (29).

Meanwhile, in the limit of $\nu_s \gg g$, the counter rotating terms in H can be neglected and the effective Hamiltonian of the hybrid array is reduced to

$$H = (\nu_s - 2g)\sum_j s_j^\dagger s_j - g\sum_j (s_j^\dagger s_{j+1} + s_{j+1}^\dagger s_j). \tag{30}$$

This Hamiltonian corresponds to the tight-binding model of bosons on a 1D lattice. We can diagonalize the Hamiltonian as

$$H = \sum_k E_k b_k^\dagger b_k, \tag{31}$$

where

$$E_k = \nu_s - 2g(1+\cos k). \tag{32}$$

This dispersion relation agrees with Eq. (27), in the limit of $\nu_s \gg g$:

$$\begin{aligned} E_k &= \nu_s \Big[1 - \frac{4g}{\nu_s}(1+\cos k)\Big]^{1/2} \\ &\approx \nu_s \Big[1 - \frac{2g}{\nu_s}(1+\cos k)\Big] \\ &= \nu_s - 2g(1+\cos k). \end{aligned} \tag{33}$$

Similar to the energy bands of non-interacting electrons in a crystal, the dispersion relation in Eq. (32), determines an energy band of the 1D bosonic crystal.

V. DISCUSSION AND CONCLUSION

Compared with the scheme composed solely of superconducting qubits, our proposed hybrid system can be more easily tuned to the ultrastrong-coupling regime. Experimentally, this can be conveniently achieved by tuning the applied magnetic field to increase the ratio of the coupling strength between the flux qubit and the NV-center ensemble to the excitation frequency of the spin ensemble. As given in Sec. II, for the experimentally accessible parameters $I_p = 0.9$ μA, $a = 2$ μm, and $b = 50$ μm, the coupling strength J between the flux qubit and the NV-center ensemble can be as strong as $J \sim 250$ MHz. If the frequency of the NV-center ensemble is tuned, for example, to $\nu_s \sim 1$ GHz via the external magnetic field, one can reach an ultrastrong-coupling regime with $J/\nu_s \sim 25\%$. The corresponding ratio of the effective coupling strength g between bosons to the excitation frequency of the spin ensemble can reach $g/\nu_s \sim 12\%$. However, in the well-established scheme composed solely of superconducting qubits [45], where two flux qubits are coupled via an additional large-detuned flux qubit, the ratio of the effective coupling strength between the two flux qubits to the single-qubit frequency is about 1.5%. Obviously, it is much smaller than the achievable ratio $g/\nu_s \sim 12\%$ in our hybrid system.

Coherence times in superconducting qubits have been steadily increasing over the past decade, with the coherence times in excess of 100 μs for the transmon qubit in a 3D cavity [49, 50]. Due to the large capacitance shunted to the qubit, the effect of the charge noise on the qubit is greatly suppressed. Also, it is this large shunt capacitance that yields a strong coupling between the qubit and the cavity. However, it is hard to use only one qubit to both simultaneously and strongly couple two cavities, due to the difficulty in circuits design. Also, it could be a similar case for the proposed 1D array of resonators coupled by either superconducting-ring couplers or dc-SQUIDs [51], because it is usually not easy to achieve ultrastrong couplings for a superconducting-ring coupler (dc-SQUID) simultaneously coupled to two resonators. In contrast, as discussed above, our proposed hybrid system can be more conveniently tuned to the ultrastrong-coupling regime by just tuning the applied magnetic field to increase the ratio of the qubit-spin coupling to the excitation frequency of the spin ensemble.

In a coupled system, it is difficult to directly calculate the relaxation or decoherence times of the subsystems because they depend on the nature of the environment coupled to each subsystem. However, they can be estimated from some experimental observations. For instance, in a recent experiment on the hybrid system consisting of a flux qubit and a NV-center ensemble, it was estimated from the observed decay time of the quantum oscillations that, when the flux qubit was in resonance with the NV centers, the relaxation times were $T_{1,\rm qb} \sim 150$ ns for the flux qubit and $T_{1,\rm NV} \gg 10$ μs for the NV centers [30]. In our proposed hybrid system, the flux qubit is kept in the ground state, so the coherence times of the NV centers should be even longer since the designed off-resonance of the flux qubit to the NV centers will suppress the deco-

herence on the NV centers induced by the relaxation of the flux qubit. In fact, in our proposed hybrid system, the flux qubit is largely detuned from the NV centers. Typically, the frequency ν_q of the flux qubit can be designed as 5-10 GHz. In the experiments of superconducting qubits, the temperature can be as low as $T \sim 10$ mK, which corresponds to $k_B T \sim 0.1$ GHz $\ll \nu_q$. Thus, even a lossy flux qubit can indeed be kept in the ground state at such a low temperature, and its relaxation-induced decoherence on the NV centers is then suppressed.

In conclusion, we have studied a hybrid quantum system consisting of spin ensembles and superconducting flux qubits. Each spin ensemble is realized using the NV centers in a diamond crystal, and every two nearest-neighbor spin ensembles are effectively coupled by adiabatically eliminating the degrees of freedom of the flux qubit placed in between these two spin ensembles. The coupling strengths between flux qubits and spin ensembles can be tuned into strong- and even ultrastrong- coupling regimes by either engineering the hybrid structure in advance or tuning the excitation frequencies of spin ensembles via the external magnetic fields. As an elementary structure, three effectively coupled spin ensembles can be used to simulate the system of coupled bosons, especially for demonstrating bilinear coupling between bosons in the ultrastrong-coupling regime. Moreover, due to the advantage of scalability, this structure can be extended to construct hybrid arrays to simulate 1D bosonic lattices with tunable coupling strengths. In the strong-coupling regime, the hybrid array can be simply reduced to the tight-binding model on a 1D bosonic lattice. However, in the ultrastrong-coupling regime, the hybrid array exhibits more interesting properties. Because of the bilinear coupling in this regime, it can exhibit quasi-particle excitations that have an energy gap from the ground state. Moreover, these quasi-particle excitations and the ground state are stable under a certain condition that is tunable via the external magnetic field.

ACKNOWLEDGMENTS

This work is supported by the National Natural Science Foundation of China Grant No. 91121015, the National Basic Research Program of China Grant No. 2014CB921401, and the NSAF Grant No. U1330201. L.T. is supported by the National Science Foundation under Awards No. 0956064 and No. 0916303.

[1] I. Buluta, and F. Nori, Science **326**, 108 (2009); I. M. Georgescu, S. Ashhab, and F. Nori, Rev. Mod. Phys. 86 , 153 (2014) and references therein.
[2] A. Retzker, R. C. Thompson, D. M. Segal, and M. B. Plenio, Phys. Rev. Lett. **101**, 260504 (2008).
[3] D. Jaksch and P. Zoller, Ann. Phys. (N.Y.) **315**, 52 (2005).
[4] A. Micheli, G. K. Brennen, and P. Zoller, Nat. Phys. **2**, 341 (2006).
[5] S. L. Sondhi, S. M. Girvin, J. P. Carini, and D. Shahar, Rev. Mod. Phys. **69**, 315 (1997).
[6] J. Q. You, X. F. Shi, X. Hu, and F. Nori, Phys. Rev. B **81**, 014505 (2010).
[7] I. Bloch, T. W. Hänsch, and T. Esslinger, Nature (London) **403**, 166 (2000).
[8] J. K. Chin, D. E. Miller, Y. Liu, C. Stan, W. Setiawan, C. Sanner, K. Xu, and W. Ketterle, Nature (London) **443**, 961 (2006).
[9] J. Simon, W. S. Bakr, R. Ma, M. E. Tai, P. M. Preiss, and M. Greiner, Nature (London) **472**, 307 (2011).
[10] J. Struck, C. Ölschläger, R. Le Targat, P. Soltan-Panahi, A. Eckardt, M. Lewenstein, P. Windpassinger, and K. Sengstock, Science **333**, 996 (2011).
[11] A. Friedenauer, H. Schmitz, J. T. Glückert, D. Porras, and T. Schätz, Nat. Phys. **4**, 757 (2008).
[12] K. Kim, M. S. Chang, S. Korenblit, R. Islam, E. E. Edwards, J. K. Freericks, G. D. Lin, L. M. Duan, and C. Monroe, Nature (London) **465**, 590 (2010).
[13] R. Amsüss, C. Koller, T. Nöbauer, S. Putz, S. Rotter, K. Sandner, S.Schneider, M. Schramböck, G. Steinhauser, H. Ritsch, J. Schmiedmayer, and J. Majer, Phys. Rev. Lett. **107**, 060502 (2011).
[14] Y. Kubo, C. Grezes, A. Dewes, T. Umeda, J. Isoya, H. Sumiya, N. Morishita, H. Abe, S. Onoda, T. Ohshima, V. Jacques, A. Dréau, J. F. Roch, I. Diniz, A. Auffeves, D. Vion, D. Esteve, and P. Bertet, Phys. Rev. Lett. **107**, 220501 (2011).
[15] Y. Kubo, F. R. Ong, P. Bertet, D. Vion, V. Jacques, D. Zheng, A. Dréau, J. F.Roch, A. Auffeves, F. Jelezko, J. Wrachtrup, M. F. Barthe, P. Bergonzo, and D. Esteve, Phys. Rev. Lett. **105**, 140502 (2010).
[16] D. I. Schuster, A. P. Sears, E. Ginossar, L. DiCarlo, L. Frunzio, J. J. L. Morton, H. Wu, G. A. D. Briggs, B. B. Buckley, D. D. Awschalom, and R. J. Schoelkopf, Phys. Rev. Lett. **105**, 140501 (2010).
[17] A. Imamoğlu, Phys. Rev. Lett. **102**, 083602 (2009).
[18] P. Rabl, D. DeMille, J. M. Doyle, M. D. Lukin, R. J. Schoelkopf, and P. Zoller, Phys. Rev. Lett. **97**, 033003 (2006).
[19] J. Verdu, H. Zoubi, C. Koller, J. Majer, H. Ritsch, and J. Schmiedmayer, Phys. Rev. Lett. **103**, 043603 (2009).
[20] J. H. Wesenberg, A. Ardavan, G. A. D. Briggs, J. J. L. Morton, R. J. Schoelkopf, D. I. Schuster, and K. Molmer, Phys. Rev. Lett. **103**, 070502 (2009).
[21] Z. L. Xiang, X. Y. Lü, T. F. Li, J. Q. You, and F. Nori, Phys. Rev. B **87**, 144516 (2013).
[22] X. Y. Lü, Z. L. Xiang, W. Cui, J. Q. You, and F. Nori, Phys. Rev. A **88**, 012329 (2013).
[23] Z. L. Xiang, S. Ashhab, J. Q. You, and F. Nori, Rev. Mod. Phys. **85**, 623 (2013).
[24] W. L. Yang, Z. Q. Yin, Z. X. Chen, S. P. Kou, M. Feng, and C. H. Oh, Phys. Rev. A **86**, 012307 (2012).
[25] L. Chotorlishvili, D. Sander, A. Sukhov, V. Dugaev, V. R. Vieira, A. Komnik, and J. Berakdar, Phys. Rev. B **88**,

085201 (2013).
[26] P. Rabl and P. Zoller, Phys. Rev. A **76**, 042308 (2007).
[27] K. Tordrup, A. Negretti, and K. Mølmer, Phys. Rev. Lett. **101**, 040501 (2008).
[28] D. Petrosyan, G. Bensky, G. Kurizki, I. Mazets, J. Majer, and J. Schmiedmayer, Phys. Rev. A **79** , 040304 (2009).
[29] D. Marcos, M. Wubs, J. M. Taylor, R. Aguado, M. D. Lukin, and A. S. Sørensen, Phys. Rev. Lett. **105**, 210501 (2010).
[30] X. Zhu, S. Saito, A. Kemp, K. Kakuyanagi, S. Karimoto, H. Nakano, W. J. Munro, Y. Tokura, M. S. Everitt, K. Nemoto, M. Kasu, N. Mizuochi, and K. Semba, Nature (London) **478**, 221 (2011).
[31] J. E. Hoffman, J. A. Grover, Z. Kim, A. K. Wood, J. R. Anderson, A. J. Dragt, M. Hafezi, C. J. Lobb, L. A. Orozco, S. L. Rolston, J. M. Taylor, C. P. Vlahacos, and F. C. Wellstood, Rev. Mex. Fís. **57**, 1 (2011).
[32] T. Hümmer, G. M. Reuther, P. Hänggi, and D. Zueco, Phys. Rev. A **85**, 052320 (2012).
[33] M. J. Hartmann, F. G. Brandao, and M. B. Plenio, Nat. Phys. **2**, 849 (2006).
[34] A. D. Greentree, C. Tahan, J. H. Cole, and L. C. L. Hollenberg, Nat. Phys. **2**, 856 (2006).
[35] D. G. Angelakis, M. F. Santos, and S. Bose, Phys. Rev. A **76**, 031805 (2007).
[36] M. Leib and M. J. Hartmann, New J. Phys. **12**, 093031 (2010).
[37] S. Schmidt, D. Gerace, A. A. Houck, G. Blatter, and H. E. Türeci, Phys. Rev. B **82**, 100507 (2010).
[38] T. P. Orlando, J. E. Mooij, L. Tian, Caspar H. van der Wal, L. S. Levitov, S. Lloyd, and J. J. Mazo Phys. Rev. B **60**, 15398 (1999).
[39] P. Neumann, R. Kolesov, V. Jacques, J. Beck, J. Tisler, A. Batalov, L. Rogers, N. B. Manson, G. Balasubramanian, F. Jelezko, and J. Wrachtrup, New. J. Phys. **11**, 013017 (2009).
[40] J. B. Majer, F. G. Paauw, A. C. J. ter Haar, C. J. P. M. Harmans, and J. E. Mooij, Phys. Rev. Lett. **94**, 090501 (2005).
[41] E. H. Lieb and W. Liniger, Phys. Rev. **130**, 1605 (1963).
[42] C. P. Sun, Y. Li, and X. F. Liu, Phys. Rev. Lett. **91**, 147903 (2003).
[43] V. M. Acosta, E. Bauch, M. P. Ledbetter, C. Santori, K. M. C. Fu, P. E. Barclay, R. G. Beausoleil, H. Linget, J. F. Roch, F. Treussart, S. Chemerisov, W. Gawlik, and D. Budker, Phys. Rev. B **80**, 115202 (2009).
[44] F. G. Paauw, A. Fedorov, C. J. P. M. Harmans, and J. E. Mooij, Phys. Rev. Lett. **102**, 090501 (2009).
[45] A. O. Niskanen, K. Harrabi, F. Yoshihara, Y. Nakamura, S. Lloyd, and J. S. Tsai, Science **316**, 723 (2007).
[46] H. Fröhlich, Phys. Rev. 79, 845 (1950); Proc. R. Soc. London, Ser. A **215**, 291 (1952).
[47] S. Nakajima, Adv. Phys. **4**, 363 (1953).
[48] A. O. Niskanen, Y. Nakamura, and J. S. Tsai, Phys. Rev. B **73**, 094506 (2006).
[49] H. Paik, D. I. Schuster, L. S. Bishop, G. Kirchmair, G. Catelani, A. P. Sears, B. R. Johnson, M. J. Reagor, L. Frunzio, L. I. Glazman, S. M. Girvin, M. H. Devoret, and R. J. Schoelkopf, Phys. Rev. Lett. **107**, 240501 (2011).
[50] C. Rigetti, J. M. Gambetta, S. Poletto, B. L. T. Plourde, J. M. Chow, A. D. Córcoles, J. A. Smolin, S. T. Merkel, J. R. Rozen, G. A. Keefe, M. B. Rothwell, M. B. Ketchen, and M. Steffen, Phys. Rev. B **86,** 100506(R) (2012).
[51] B. V. Correa, A. Kurcz and J. J. García-Ripoll, J. Phys. B **46,** 224024 (2013).